Research on the field emission mechanism of nano-structured carbon film*

Wang Yan-Yan(王艳燕)[a], Li Ying-Ai(李英爱)[b],
Xu Ji-Song(许基松)[a], and Gu Guang-Rui(顾广瑞)[a]†

[a] *Department of Physics, College of Science, Yanbian University, Yanji* 133002, *China*
[b] *National Laboratory of Superhard Materials, Jilin University, Changchun* 130012, *China*

(Received 9 January 2012; revised manuscript received 15 February 2012)

The field emission (FE) characteristics of nano-structured carbon films (NSCFs) are investigated. The saturation behaviour of the field emission current density found at high electric field E cannot be reasonably explained by the traditional Fowler–Nordheim (F–N) theory. A three-region E model and the curve-fitting method are utilized for discussing the FE characteristics of NSCFs. In the low, high, and middle E regions, the FE mechanism is reasonably explained by a modified F–N model, a corrected space-charge-limited-current (SCLC) model and the joint model of F–N and SCLC mechanism, respectively. Moreover, the measured FE data accord well with the results from our corrected theoretical model.

Keywords: nano-structured carbon films, field emission, F–N theory, space charge limited current, three-region electric field model

PACS: 79.70.+q, 81.05.U–, 81.15.Gh **DOI:** 10.1088/1674-1056/21/8/087902

1. Introduction

Carbon material has attracted considerable attention because of its good electron field emission (FE) properties with low threshold electric field (E)[1] and high FE current density[2] in recent years. Many reports indicate that amorphous carbon film is a promising candidate for the field emitters because of its unique chemical, electrical, optical and mechanical properties. Therefore, most of the previous work has focused on various nano-carbon films. Zheng *et al.*[3] obtained the enhanced field-emission properties of carbon nanotubes by magnetically controlled nickel-electroplating treatment.[3] Wang *et al.* found that the good FE properties of carbon nano-sheets[4] and carbon nanoflakes[5] might be due to the high density of graphite edges which had a number of potential emission sites. Wang *et al.*[6] studied the FE characteristics of other nano-carbon films.

Many recent studies indicate that the FE current of the nano-carbon film has a saturated trend which cannot be reasonably explained in terms of the classic F–N theory.[1,2,7] The classic F–N theory should be adapted to the case of a flat cathode surface of metal with a sufficient number of free electrons. It may not be applicable for various carbon nanofilms that have complex structures with irregular shapes and their emission sites and electrical conductivities are significantly different from those of pure metal plates. Moreover, the number of FE sites and parameters may not be constant when a high electric field of about 10^7 V/cm is applied to samples.[8] Under an extremely high electric field, the FE current can be limited by the space-charge-limited-current (SCLC) effect, screening effect,[2] and so on.

Many explanations on the FE mechanism of carbon nanofilm are based on the F–N theory, but the saturation trend of the FE current in the high E region is not clearly interpreted. No complete theory can be used to explain the FE mechanism of carbon nanofilm. Therefore, it is very important to explore the FE mechanism of carbon nanofilm in application to the field emission electron source with high current. We studied the FE properties of nano-sheet and nano-needle carbon films,[9−13] and suggested a three-region E model to explain the FE characteristics.[13] In this study, in order to further understand the FE mechanism of nano-structured carbon film (NSCF), a

*Project supported by the National Natural Science Foundation of China (Grant No. 11164031) and the Scientific Research Foundation for the Returned Overseas Chinese Scholars, Ministry of Education of China (Grant No. (2009)1341).

†Corresponding author. E-mail: grgu@ybu.edu.cn

© 2012 Chinese Physical Society and IOP Publishing Ltd

three-region E model is explained in detail, and the further modification and discussion for our model in the low, middle, and high E regions are performed.

2. Three-region E model

If we assume that the distribution of emitter tip radii on a carbon film surface is a Gaussian distribution, the height of every emitter is constant, and the FE behaviours of these tips are determined by their geometry field enhancement factors, then the FE current of few emitters which yield a smaller tip radius will become saturation even if in a relatively low E region. In this case, these emitters are named saturated emitters; other emitters are named un-saturated emitters. Thus, the FE behaviour of carbon film is governed by un-saturated emitters and saturated emitters at an applied field. According to Gaussian distribution, in a relatively low E region, the number of saturated emitters is small and the radii of these emitters are also very small; therefore, the contribution to total FE current of carbon films from these emitters can be neglected. On the other hand, as E increases, the number and the radii of saturated emitters become large, thus, the contribution to total FE current from these emitters becomes more and more important; at this time, the total FE current can be divided into the saturated part (from saturated emitters) and the un-saturated part (from un-saturated emitters). If E becomes strong enough, the FE behaviour of carbon film will be controlled by saturated emitters, and then the contribution to total FE current from un-saturated emitters can be neglected.

So, the FE behaviour will be divided into different E regions in order to more clearly explain the FE characteristics of NSCFs. Here, as an example, the nano-carbon needle films (NCNFs) deposited by microwave plasma chemical vapour deposition[9] are discussed. Figure 1 shows a typical FESEM image of the NCNF. As shown in Fig. 1, we are able to estimate the mean height (H), diameter (d_0), and density (n) of needles to be about 4 μm, 0.3 μm, and 10^6 mm^{-2}, respectively.

A typical FE current density–electric field (J–E) curve measured by the prevenient device [9−13] is plotted in Fig. 2. As shown in Fig. 2, field emission current density (J) steeply increases with E increasing at $E \lessapprox 3.3$ V/μm, above which there appears an obvious saturation behaviour in J. The maximum J of 67.0 mA/cm^2 is attained at $E = 10$ V/μm. The measured FE data of the NCNF will be discussed separately in the three E regions[13] according to our experimental data as follows. (i) A low E region (unsaturated J region, $E \lessapprox 3.3$ V/μm), where the FE behaviour is controlled mainly by unsaturated emitters and follows the F–N theory. (ii) A middle E region (partly-saturated J region, 3.3 V/μm$\lessapprox E \lessapprox$ 4 V/μm), where the FE behaviour is determined by both partially un-saturated emitters and partially saturated emitters and abides partially by the F–N theory. (iii) A high E region (fully-saturated J region, $E \gtrapprox 4$ V/μm), where all the emitters become saturated and the FE behaviour completely disaccords with F–N theory.

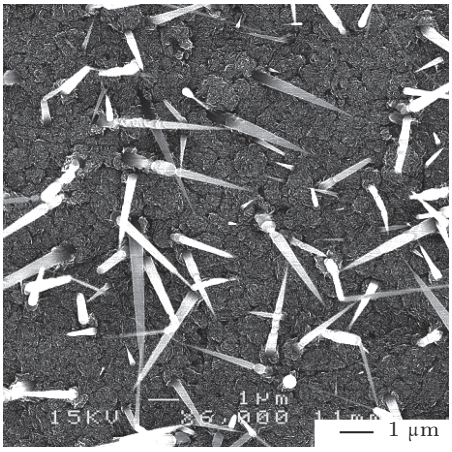


Fig. 1. The SEM image of a typical nano-carbon needle film.

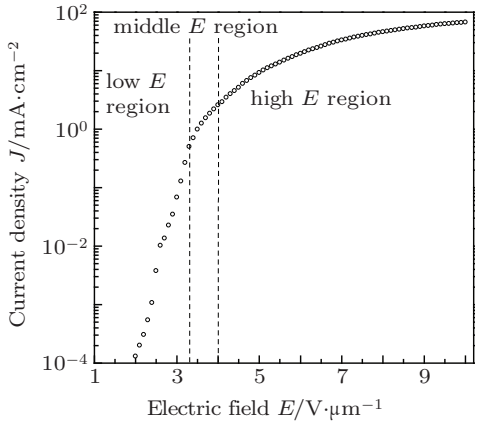


Fig. 2. The FE J–E data incorporating into three electric field regions.

3. Results and discussion

3.1. FE mechanism in the low E region

In the low E region, the following assumptions are made: i) the field emission behaviours of all unsaturated emitters follow the traditional F–N theory;

ii) the work function of each emitter, ϕ, is a constant; iii) the height of each emitter, H, is constant, while their tip radius, r, varies according to a Gaussian distribution on the carbon film's surface; iv) the emitter density, n, may change with electric field, but approximately is a constant value in a smaller sector. In addition, FE occurs from the surface of each emitter tip whose area is $s = \pi r^2$.

According to the classical F–N theory, total emission current density is given by

$$J = \frac{A}{\phi t(y)} F^2 \exp\left[-B\frac{\phi^{3/2}}{F} v(y)\right], \tag{1}$$

where F is a local electric field on emitter tip surface, constants A and B are combinations of electron charge (e), mass (m), and Planck's constant h. In the un-saturated region, the function $v(y)$ and $t(y)$ may be expressed as[14]

$$\nu(y) = 0.95y - 1.03y^2, \quad t(y) = 1. \tag{2}$$

So, the total emission current density may be rewritten as

$$J = \frac{A}{\phi} F^2 \exp\left[1.03Be^3\phi^{-1/2}\right] \times \exp\left[-0.95\frac{B\phi^{3/2}}{F}\right], \tag{3}$$

where constants $A = 1.5414 \times 10^{-6}$ A·eV·V^{-2}, $B = 6.8309 \times 10^9$ eV$^{-3/2}$·V·m^{-1}, and $1.03Be^3 = 10.1$ eV.[15] The linear relationship between local field value F and applied E is generally given as

$$F = \frac{H}{r} E. \tag{4}$$

The Gaussian distribution $n(r)$ of each emitter tip radius is given by

$$n(r) = N/\sqrt{2\pi\sigma^2}\exp[-(r - r_0)^2/2\sigma^2], \tag{5}$$

where r_0 (in unit m) and σ (in unit m) are the average and standard deviation of the radius distribution of the emitted emitter tips, and N is the number of the field emitter. So, the total emission current is expressed as

$$I = \int J \mathrm{d}s = \int J\pi r^2 n(r)\mathrm{d}r. \tag{6}$$

Finally,

$$I = CNE^2 \exp[-r_0(D/E)] + \frac{\sigma^2}{2}(D/E)^2, \tag{7}$$

where $C = A\pi H^2/\varphi \exp[10.1/\sqrt{\varphi}]$ and $D = 0.95B\varphi^{3/2}/H$. So, F–N equation can be written as

$$\ln(I/V^2) = \ln(CN/d^2) - Ddr_0(1/V) + \frac{\sigma^2}{2}D^2d^2(1/V^2), \tag{8}$$

where d is the distance of the cathode and anode.

Figure 3 shows the F–N curve of the typical NCNF corresponding to the J–E plot shown in Fig. 2. As shown in Fig. 3, FE data are fitted to a quadratic equation given by $y = a + bx + cx^2$ in the low E region. Parameters a, b, and c can be obtained by comparing Eq. (8) as follows:

$$a = \ln(CN/d^2), \quad b = -Dr_0 d, \quad c = \frac{\sigma^2}{2}D^2d^2. \tag{9}$$

It can be inferred as

$$\frac{\sigma^2}{2r_0^2} = \frac{c}{b^2}, \quad H^2 = \frac{\phi d^2\, \mathrm{e}^{a-10.1/\sqrt{\phi}}}{A\pi N}, \quad r_0 = \frac{b\,\mathrm{e}^{(a-10.1/\sqrt{\phi})/2}}{0.95\pi^{1/2}N^{1/2}A^{1/2}B\phi}. \tag{10}$$

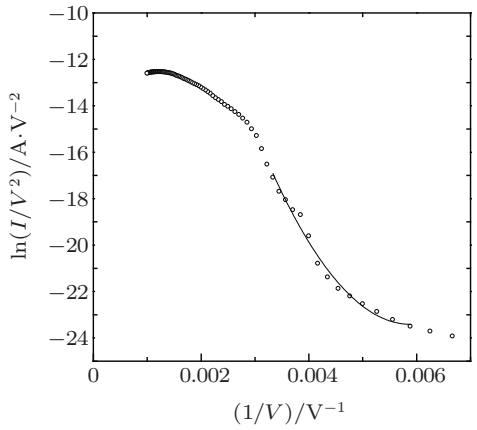


Fig. 3. The F–N curve fitting to a quadratic equation in the low E region.

The calculation results of $r_0 = 0.28$ μm and $H = 4.16$ μm are consistent with the observed values taken from the FESEM. Meanwhile, the values of C and D can be estimated to be 1.568×10^{-3} and 1.73×10^8 from Eq. (9), respectively.

Figure 4 shows the J–E curves taken from measured FE data and the fitted curve taken from Eq. (7) in the low E region. As shown in Fig. 4, the experimental data in the low electric field region can be well consistent with the results from our modified F–N equation. In other words, the FE mechanism in

the low E region can be reasonably explained by the modified F–N model.

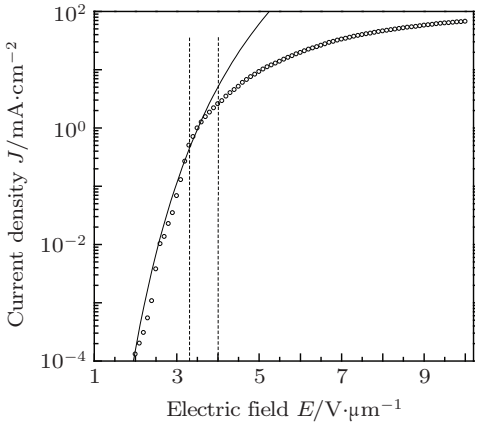


Fig. 4. The J–E curve and the fitting curve taken from the modified F–N model in the low E region.

3.2. FE mechanism in the high E region

Figure 4 shows that there is an obvious deviation between the F–N theory curve and experimental data when E is more than about 3.3 V/μm, which is coincident with our previous experimental result.[9] So, in the high E region, FE data cannot be interpreted by the F–N theory. A substantial contribution of a space-charge-limited-current (SCLC) mechanism should be considered to explain the FE behaviour observed in the sufficiently high E region, because the field enhancement effect of each FE emitter may not work fully at such a high E due to an insufficient screening effect by a limited number of free electrons. In such a case, according to the Child–Langmuir law,[16,17] the SCLC density, $J_{\rm SC}$, in the high E region is given by

$$\begin{aligned} J_{\rm SC} &= (16\pi\varepsilon_0/9)(2e/m)^{1/2}(U^{3/2}/d^2) \\ &= C_{\rm SC}(U^{3/2}/d^2) = C_{\rm SC}\pi(E^{3/2}/d^{1/2}), \\ C_{\rm SC} &= (16\pi\varepsilon_0/9)(2e/m)^{1/2}. \end{aligned} \tag{11}$$

In the present case, $E = \beta E_{\rm ap} = (H/r)E_{\rm ap}$, meanwhile it is assumed that $d \approx kr$ where k is a proportional coefficient. Thus

$$\begin{aligned} J_{\rm SC} &\approx C_{\rm SC}(H/r)^{3/2}E_{\rm ap}^{3/2}/d^{1/2} \\ &= C_{\rm SC}H^{3/2}E_{\rm ap}^{3/2}/(k^{1/2}r^2). \end{aligned} \tag{12}$$

The emission area can be expressed as $N\pi r^2$ in our model, so the emission current is expressed as

$$I_{\rm SC} = K_{\rm SC}E_{\rm ap}^{3/2}, \tag{13}$$

where

$$K_{\rm SC} = C_{\rm SC}\pi NH^{3/2}/k^{1/2}. \tag{14}$$

In order to tally well with experimental data, it is modified as follows by considering the local electric field enhancement effect and the nanostructure of the NCNF:

$$I_{\rm SC} = K_{\rm SC}(E - E_{\rm th})^{3/2}, \tag{15}$$

where $E_{\rm th}$ should be considered as an excited electric field of the space charge effect. Here, $E_{\rm th}$ can be 3.3 V/μm according to our three-E region model. So, the theoretical values of $K_{\rm SC}$ can be estimated to be about 4.3.

As a matter of fact, the measured FE data can be well fitted only at $E \gtrapprox 4.0$ V/μm by using Eq. (15) as shown in Fig. 5. This means that the SCLC model can be a strong candidate for the mechanism explaining the saturated behaviour observed at the high FE currents. Namely, the FE mechanism in the high E region can be reasonably explained by the modified SCLC model.

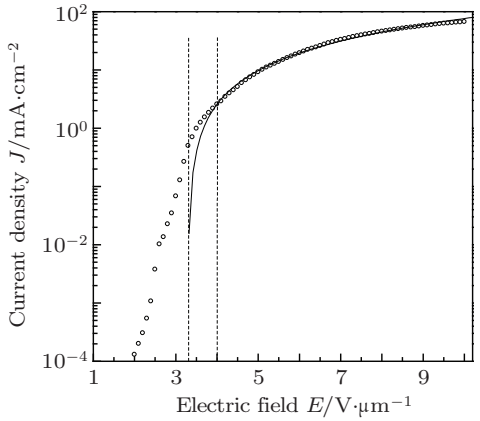


Fig. 5. The J–E curve and the fitting curve taken from the corrected SCLC model in the high E region.

3.3. FE mechanism in the middle E region

In order to facilitate discussion, we denote the FE current which obeyed the F–N mechanism as $I_{\rm FN}$ in the low E region. In the middle E region, there is not a simple model that can explain the FE mechanism of the NCNF. Thus, we consider that the FE current in the middle E region should be a combination of $I_{\rm FN}$ obtained from F–N mechanism and $I_{\rm SC}$ obtained SCLC mechanism. Therefore, the emission current in the middle E region can be given as

$$I = k_1 I_{\rm FN} + k_2 I_{\rm SC}, \tag{16}$$

where k_1 and k_2 are the introduced parameters satisfying

$$0 \le k_1 \le 1, \quad 0 \le k_2 \le 1. \tag{17}$$

Figure 6 shows the fitted curve of measured J–E data in the middle E region by using Eq. (16). Here, we assume that k_1 (k_2) changes with E increasing in a range from 1 to 0 (from 0 to 1) and two parameters satisfy a linear relation given by $k_1 + k_2 = 1$. According to the three-E region model, k_2 can be taken from J–E data as

$$k_2 = (X - 3.3)/(4.0 - 3.3), \tag{18}$$

where the parameter X changes in a range from 3.3 to 4.0 with E increasing in our model.

As shown in Fig. 6, it is observed that the fitted curve is basically consistent with the experimental data in the middle E region. In other words, the FE characteristics can be explained by the joint model of F–N and SCLC mechanism in the middle E region. So, the FE behaviour in the middle E region can be understood as follows. In the middle E region, when a relatively low E is applied to the sample, the FE behaviour is governed mainly by the F–N mechanism. With E increasing, the influence of the F–N mechanism on the FE behaviour is gradually weakened whereas the influence of the SCLC mechanism is gradually enhanced. Finally, the FE behaviour is completely governed by the SCLC mechanism and the transition into the high E regions takes place.

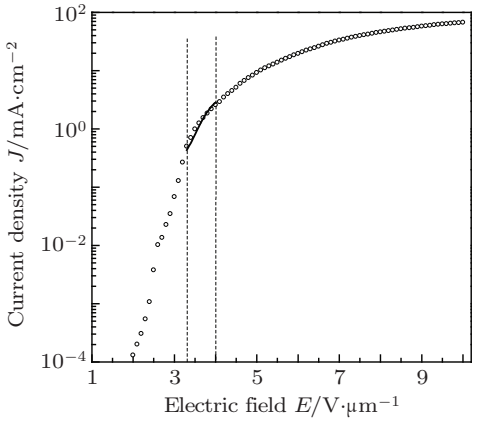


Fig. 6. The J–E curve and the fitting curve taken from the conjunct model controlled by the F–N and SCLC mechanism in the middle E region.

4. Conclusion

Taking the nano-carbon needle film for example, the field emission (FE) mechanism of nano-structured carbon films (NSCFs) is successfully discussed by the three-region electric field (E) model in which the FE data are divided into the low, middle, and high E regions. The FE characteristics of NSCFs in the low E region are reasonably explained by the modified F–N model written as

$$I_{\rm FN} = CNE^2 \exp\left[-r_0 d/D + \frac{\sigma^2}{2}(D/E)^2\right]$$

considering the statistical effect of the distribution of field emitters. The discussion indicates that the corrected space charge limited current (SCLC) model expressed as $I_{\rm SC} = K_{\rm SC}(E - E_h)^{3/2}$ in terms of the Child–Langmuir law is a strong candidate for explaining the FE mechanism of NSCFs in the high E region. In the middle E region, the model given by $I = k_1 I_{\rm FN} + k_2 I_{\rm SC}$ considering the conjunct contribution of $I_{\rm FN}$ controlled by the F–N mechanism and $I_{\rm SC}$ controlled by the SCLC mechanism is obtained, consequently the field emission data are reasonably explained.

References

[1] Li J J, Gu C Z, Wang Q, Xu P, Wang Z L, Xu Z and Bai X D 2005 *Appl. Phys. Lett.* **87** 143107
[2] Wang J, Teraji T and Ito T 2005 *Diamond Relat. Mater.* **14** 2074
[3] Zheng L W, Hu L Q, Xiao X J, Yang F, Lin H and Guo T L 2011 *Chin. Phys.* B **20** 128502
[4] Wang J J, Zhu M Y, Outlaw R A, Zhao X, Manos D M, Holloway B C and Mammana V P 2004 *Appl. Phys. Lett.* **85** 1265
[5] Wang J J, Zhu M Y, Zhao X, Outlaw R A, Manos D M, Holloway B C and Park C 2004 *J. Vac. Sci. Technol.* B **22** 1269
[6] Wang W H, Lin Y T and Kuo C T 2005 *Diamond Relat. Mater.* **14** 907
[7] Bonard J M, StÖckli T, Maier F, Heer de W A and Chatelain A 1998 *Phys. Rev. Lett.* **81** 1441
[8] Liu X, Zhu C and Li Y 2004 *Physica* B **344** 243
[9] Gu G R and Ito T 2008 *Diamond Relat. Mater.* **17** 817
[10] Gu G R, Jin Z and Ito T 2008 *Chin. Phys.* B **17** 1467
[11] Gu G R and Ito T 2009 *Chin. Phys.* B **18** 4547
[12] Gu G R and Ito T 2011 *Appl. Surf. Sci.* **257** 2455
[13] Wang J, Li Y A, Gu G R and Ito T 2011 *Vacuum* **86** 356
[14] Gomer R 1993 *Field Emission and Field Ionization* (New York: American Institute of Physics)
[15] Wang J and Ito T 2007 *Diamond Relat. Mater.* **16** 364
[16] Child C D 1911 *Phys. Rev.* **32** 492
[17] Langmuir I 1923 *Phys. Rev.* **21** 419